Proceedings of the ASME 2013 International Design Engineering Technical Conferences & Computers and Information in Engineering Conference
IDETC/CIE 2013
August 4-7, 2013, Portland, USA

DETC2013-13318

MASSIVELY PARALLEL DISCRETE ELEMENT MODELING OF WHEELED MOBILITY ON GRANULAR TERRAIN *

Ryan Houlihan
Summer Intern at Mobility and Robotics Systems Section
Jet Propulsion Laboratory
California Institute of Technology
4800 Oak Grove Drive, Pasadena CA 91109
Email: ryan.houlihan90@gmail.com

Rudranarayan Mukherjee
Mobility and Robotics Systems Section
Jet Propulsion Laboratory
California Institute of Technology
4800 Oak Grove Drive, Pasadena CA 91109
Email: Rudranarayan.M.Mukherjee@jpl.nasa.gov

ABSTRACT

Quantitatively understanding wheeled mobility on granular terrain such as sand or gravel is critical for design and operations of ground vehicles for terrestrial or extra-terrestrial applications. While the Bekker-Wong theory of wheeled mobility and its derivatives have been used in many applications, the static nature of these formulations are limiting in understanding mobility in deformable terrain under dynamic mobility conditions. Single wheel hardware experiments in laboratory settings and detailed modeling of wheel-terrain interactions are two avenues currently being actively pursued to develop quantitative understanding of wheeled mobility. In this paper, we present findings of massively parallel discrete element modeling of wheeled mobility on granular media such as sand. We present a brief overview of the underlying methodology and then focus on the results of the simulation. In these simulations, we model the inter-granular interactions and interactions between the wheel and the granules with an objective of using high fidelity first-principles approach to capture emergent behavior in these complex and highly dynamic phenomena. These simulations typically model millions of granules and use highly scalable software and parallel computing resources to overcome the severe complexity of the problem. We present results of parametric studies with varying levels of both wheel penetration and mobility conditions. These have been modeled to present a quantitative perspective of the diverse behaviors encountered in wheeled mobility on granular terrain. We have retained the full complexity of the problem by simulating granules of the size encountered in real terrain to overcome the fidelity limited issues of other comparable methods that use much larger granules.

INTRODUCTION

Quantifying mobility of unmanned ground vehicles in natural terrain is essential for their robust design and dynamic operations. Many of the natural terrain encountered in terrestrial applications can be classified as terrain made of compacted granular terrain. For extra terrestrial applications, Martian, Lunar and small body terrains are primarily granular in nature. Unlike on-road mobility, natural terrain poses interesting challenges in quantifying or predicting mobility performance as the terrain is subject to deformations and has artifacts such as various levels of compaction, slopes, moisture content and heterogeneity in composition. Consequently, robotic mobility on granular terrain has become an active area of research.

Experimentally, there are two options often pursued. One is full vehicle testing where the robotic vehicle is driven over natural terrain and its ability to traverse the terrain is measured. This avenue provides binary go / no-go as well as interesting measurable quantities such as vehicle attitude, rut depths, and slip among others. While often pursued, this method results in full coupling between the terrain mechanics and vehicle dynamics and is often difficult to use as a means of segregating the ef-

*REFER TO COVER PAGE FOR DISTRIBUTION STATEMENT

fects of different parameters on mobility. Consequently, results obtained through this type of testing are difficult to extrapolate parametrically and hence raise significant uncertainties on their predictive basis. However, this is a robust means of quantifying mobility if the types of terrains in which the vehicle is expected to traverse are limited in variability or tests are conducted on all types of terrains to be encountered.

Another avenue of mobility testing that has historically been most useful in understanding parametric sensitivity of mobility is the single wheel experiment. In this, a well instrumented wheel is made to traverse over qualified man-made representations of natural terrain in a laboratory setting. For such experiments, the granular terrain simulant for the laboratory experiment is well qualified in terms of composition, compaction, moisture content etc. Similarly, the instrumentation on the wheel enables precise documentation of forward and rotational motion as well as loads arising from interactions. As this type of experiments are well-controlled, the results from these experiments are highly conducive for understanding parametric sensitivities and hence are amenable to extrapolations. New methods have emerged that use methods from optical flow such as particle image velocimetry to quantify the deformation field in the granular terrain simulant with a high degree of spatial resolution and precision. However the scope of effort, time and resources required to generate these results is considerable and have been a limiting factor.

In modeling terrain interactions, two types of methods have been traditionally pursued. One is based on using finite element based methods with a continuum approximation of the terrain. The second is based on semi-empirical (and sometimes ad-hoc) spring-damper type models. Variations of the second type range from a single point interaction to a volumetric penetration model. However, in all cases, the coefficients required for these spring-damper type force interactions are at best obtained from curve fitting experimental data or at worse generated through trial and error or heuristics that have no foundational basis. Recently, a third approach has emerged where the terrain is modeled using discrete elements and the interactions between the elements and the wheel are modeled using Hertzian type contact models or as inelastic frictional contacts. Unfortunately, a majority of these methods (if not all) attempts at using these models are typically associated with gross approximations where the terrain elements are significantly larger (sometimes several orders) than the granules found in natural granular terrain. Similarly, the terrain is modeled as a collection of uniform sized spheres. Further, due to the scale of approximations, the force interaction models between the elements, and the elements and the wheel are often treated as tunable quantities akin to the spring-damper type model. Despite the large size of elements, the uniformity of the size of the elements and the tunable force fields, good results have typically been reported. However, due to the approximations, in their current form these types of models also lack a firm predictive basis.

In this paper, we report our attempt at using discrete element method to model wheeled mobility on granular terrain. We have attempted to retain as much fidelity as possible in the simulations and have moved away from the tuning paradigm of making simulation results match experimental data. Towards this, we have modeled the terrain as a polydispersed heterogeneous medium made of elements that have the same size distribution as the granules found in natural terrain. We have also used a force interaction model where the coefficients are measurable macroscopic entities and have set these to values reported for most natural granular terrains. The results presented here are not obtained iteratively through tuning of the simulations, but from single runs to test their predictive basis. We have modeled a single wheel experimental set up and results from a parametric set of simulations are presented. Due to our effort in retaining the complexity of the physical system in the numerical simulation, we are reporting results from very large number of granules (order of several millions on an average) simulated using massively parallel DEM software and parallel computing systems.

FORCE MODEL

In our simulations granular media is modeled as a polydispersed set of spherical bodies. While in reality granules are not spherical entities the polydispersed nature of our simulation domains, with granules of various diameters, provides a good approximation. In the simulations we use three types of interaction models; (i) interactions between granules, (ii) interactions between the robotic system and the granules and (iii) interactions between simulation box walls and the granules. The simulation box walls model the effect of retaining walls in the containers used in the corresponding single wheeled experiments and CAD files represent the mechanical systems; these are both modeled as a triangular meshes. The interactions of the granules with both themselves and the triangular mesh are described in [1]. Contact is represented as described in [2]. The wall-granule, robot-granule, and granule-granule interaction forces are modeled by the Hertzian Contact Force Model as shown in equation (1).

$$\vec{F} = \sqrt{\delta} R_{\text{eff}} [(k_n \vec{\delta_{n_{ij}}} - m_{\text{eff}} \gamma_n \vec{v_n}) - (k_t \vec{\delta_{t_{ij}}} + m_{\text{eff}} \gamma_t \vec{v_t})] \qquad (1)$$

In the contact force model, δ is the scalar overlap between two particles (i and j), $\vec{\delta_{n_{ij}}}$ and $\vec{\delta_{t_{ij}}}$ are the vector components of of the overlap along the normal and tangential directions. The tangential overlap is truncated to ensure that the ratio of tangential to normal force is less than or equal to the value of the coefficient of friction μ_s defined for our material. The terms, $m_{e_{ff}}$ and R_{eff}, are the effective mass and radius of the two interacting granules where $m_{\text{eff}} = \sqrt{\frac{m_i m_j}{m_i + m_j}}$ and $R_{\text{eff}} = \sqrt{\frac{R_i R_j}{R_i + R_j}}$. All other

terms are derived from macroscopic properties of the materials themselves. Using this force model we do not allow the ad hoc specification of parameters, moving us a step away from tunable simulations where parameters can be changed to match experimental results. Instead the user can only define physically measurable parameters including; Young's modulus Y, shear modulus G, Poisson's ratio v, and coefficient of restitution e. Using these parameters and the following equations we are able to derive all necessary variables in the contact force model:

$$k_n = \frac{4}{3} Y_{\text{eff}} \sqrt{R_{\text{eff}} \delta_n} \tag{2}$$

$$\gamma_n = -2\frac{5}{6}\beta \sqrt{S_n m_{\text{eff}}} \tag{3}$$

$$k_t = 8 G_{\text{eff}} \sqrt{R_{\text{eff}} \delta_n} \tag{4}$$

$$\gamma_t = -2\frac{5}{6}\beta \sqrt{S_t m_{\text{eff}}} \tag{5}$$

$$S_n = 2 Y_{\text{eff}} \sqrt{R_{\text{eff}} \delta_n} \tag{6}$$

$$S_t = 8 G_{\text{eff}} \sqrt{R_{\text{eff}} \delta_n} \tag{7}$$

$$\beta = \frac{ln(e)}{\sqrt{ln^2(e) + \pi^2}} \tag{8}$$

$$\frac{1}{Y_{\text{eff}}} = \frac{(1-v_i^2)}{Y_i} + \frac{(1-v_j^2)}{Y_j} \tag{9}$$

$$\frac{1}{G} = \frac{2(2+v_i)(1-v_i)}{Y_i} + \frac{2(2+v_j)(1-v_j)}{Y_j} \tag{10}$$

The coefficient of friction adds a upper limit to the tangential force through $F_t = \mu_s F_n$ where F_t is the total tangential force and F_n is the total normal force. In the Hookean case tangential force between two particles grows according to a tangential spring and dashpot model unit $F_t/F_n = \mu_s$ and is then held at $F_t = F_n \mu_s$ until the particles loose contact. In our case, the Hertzian model, our forces are similar except the spring is no longer linear [3].

We can also define a coefficient of rolling friction μ_r and a cohesion energy density k. For the coefficient of rolling friction we add an additional torque contribution equal to

$$\tau_{rf} = \mu_r k_n \delta_n \frac{w_{r_{shear}}}{\|w_{r_{shear}}\|} R \tag{11}$$

where $w_{r_{shear}}$ is a projection of w_r into the shear plane where

$$w_r = \frac{r_i w_i + r_j w_j}{r_i + r_j} \tag{12}$$

and the contact radius $r_i = r_p - 0.5\delta_n$ where r_p is the particle radius.

The cohesion energy density is defined for use in the linear cohesion model. If two particles are in contact it will add an additional normal force $F = kA$ tending to maintain the contact where A is the particle contact area and k is the cohesion energy density J/m^3.

SIMULATION INFRASTRUCTURE

The simulations reported in this paper were run using a software developed in house based on open source software [3,4] that is highly parallelized and scalable. This software makes use of spatial decomposition of the simulation domain as well as high efficiency nearest neighbor sorting algorithms [5–8] to reduce computational expense. When using parallel machines spatial decomposition decomposes the simulation domain into multiple 3-dimensional sub domains which are distributed across the parallel processors. As with any method that includes deformation based force fields catastrophic energy spikes and simulation failures are possible if the appropriate temporal integration time step is not chosen. The only limitation in terms of the potential size of the simulation domain is available computational power and memory. Post process visualization is done using Paraview [9]. While results presented here were generated using polydispersed spherical granules, the software is currently capable of modeling aspherical granules that have abstract convex geometric shapes (not just ellipses or boxes). All simulations were run on one of the following two clusters. Cluster 1 is running with RedHat Linux Enterprise Edition 4.4 on the 32-bit Dell Xeon architecture. Each of the 512 compute nodes of cluster 1 runs 2 Pentium 4 Xeon processor with a clock speed of 3.2 GHz, 1 MB of cache, and 2 GB of RAM per CPU. Cluster 2 is running with SuSE 11.1 on a 64-bit Dell Xeon architecture. Each of the 152 compute nodes of cluster 2 runs 12 Intel Xeon X5650 processors with a clock speed of 2.67 GHz, 12 MB of cache, and 2 GB of RAM per CPU.

REGION DEVELOPMENT METHODOLOGIES

Creating a bed of granular media closely resembling the aggregate properties of true-to-use granular terrains is a critical step in effectively simulating wheeled mobility across a granular terrain. In creating our polydispersed granular media we resembled the statistical distribution of granule size found in natural terrain. Also macroscopic material properties used in our force model, such as Young's modulus, were set to match available material data for natural terrain. While granular size distributions and material properties are straight forward to specify in our simulation, it is not possible to define the bulk density and consequently the porosity of our granular regions as an input parameter. This is because porosity or bulk density is obtained in natural media through a gravity assisted settling process and inter-granular interaction dynamics. Towards creating a realistic bed the sim-

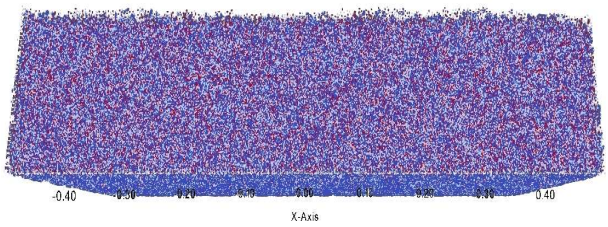

FIGURE 1. *Poly-dispersed granular region after settling under a gravity of 1 g. The coloration shows the different radii of the granules that compose the region. In total there are 1,655,064 granules in the region where the distribution of radii is as follows: 15% 2.75 mm, 10% 2.25 mm, 25% 1.75 mm, 50% 1.25 mm. When fully settled, the bulk density of the region when fully settled is 0.769 g/cm^3 with a porosity of 44% .*

ulation domain was initially discretized into a uniform grid of ghost spheres where the diameter of the ghost spheres was equal to that of the largest physical granule diameter. This is the equivalent of creating a lattice. We introduced physical granules of different sizes based on the statistical distribution of the terrain material into the ghost spheres in the lattice. While it may at first be tempting to introduce these granules in their bounding ghost spheres concentrically, this unfortunately creates an artificial regularity in the granular bed. Instead it is advantageous to randomly offset the centers of the physical granules with centers of the ghost spheres. The offset vector components can be chosen using a random number generator. This irregularity is better able to capture the heterogeneity found in natural terrain. The insertion of these granules into the ghost spheres can easily be performed concurrently and hence is amenable to highly scalable parallelization.

Initially this process will create a region of loosely packed granules with a low bulk density. By allowing the granules in the simulation domain to settle under gravity, the volume is reduced by several orders of magnitude. Once the granules have come to rest we shake the entirety of the simulation box to model compaction of the bulk material. After successive steps of mild shaking we converge to regions with bulk densities comparable to those in the true hardware experiments or natural terrain. Although this process is computational intensive for regions composed of multiple million granules, a single region of compacted granules can be reused for parametric simulations.

WHEEL ROLL SIMULATIONS

For our experiments we used a wheel represented as a cylinder. The wheel was tested at a variety of different speeds, penetration depths, static friction (μ_s) values and rolling friction (μ_r) values.

Before discussing the results of parametric simulations, consider the qualitative validation of our results against experimental data. Note that this is qualitative simulation and there are some parametric difference between the numerical and hardware set ups such as wheel diameter. Figure (2) is made of two rows. The bottom row shows results obtained from particle image velocimetery of a wheel moving on granular terrain [10]. The displacement field of the granular media is shown in color coding with red being high and blue is low. The top row shows results obtained from our numerical simulations. Here too the displacement field of the granular media is shown in the same color coding. We see parabolic curve of high velocity granules extending from the front of the wheel to the back where left is the direction of motion for both images. The bottom image also shows this very distinct parabolic curve extending from the back to the end of the wheel. Similarly, both images show a cusp or lip of the parabola as well as lower speed granules observed through the layer of green. Both images show transitions from blue to green to yellow to red in similar regions. There are some minor observable differences. These arise from our simulation not modeling the very small granules and hence the image has a fair bit of granularity as compared to the hardware experiment.

TABLE 1. *Material properties for wheel simulations. The defined properties of the wheel were also the same properties defined for the walls surrounding the region.*

Property	Granular Media	Wheel
Youngs Modulus (Pa)	5.00E+006	8.00E+011
Poissons Ratio	0.45	0.3
Coefficient of Restitution	0.75	0.75
Coefficient of Friction	0.5	0.35
Coefficient of Rolling Friction	0.4	0.3
Cohesion Energy Density (Pa)	100000	100000

For the parametric simulations, we first simulated a wheel rolling across a rectangular granular bed at various speeds and depths. For the bed we created a polydispersed region containing a total of 1,655,064 granules. The granules had a density of 2060 kg/m^3 and the distribution of granule sizes by diameter was as follows: 15% at 5.5 mm, 10% at 4.5 mm, 25% at 4.5 mm and 50% at 2.5 mm. The bulk density of the bed was 0.8792 g/cm^3 with a porosity of 57.32%. Both the wheel diameter and width is 25 cm and all simulations were run with 0% slip. Gravity was set at 9.81 m/s^2. The material properties used were the same for all experiments except for variations in our value of rolling friction and can be seen in *Table 1*. These simulations were run on approximately 180 processors for a total run time of 4-5 hours.

In the first set of simulations we investigated how changing velocities and wheel penetration depths affect the force in the horizontal (x) direction and the vertical (z) direction. The results of these simulations are shown in *Fig. 6*. We used the standard values listed in *Table 1* for all these simulations. The different

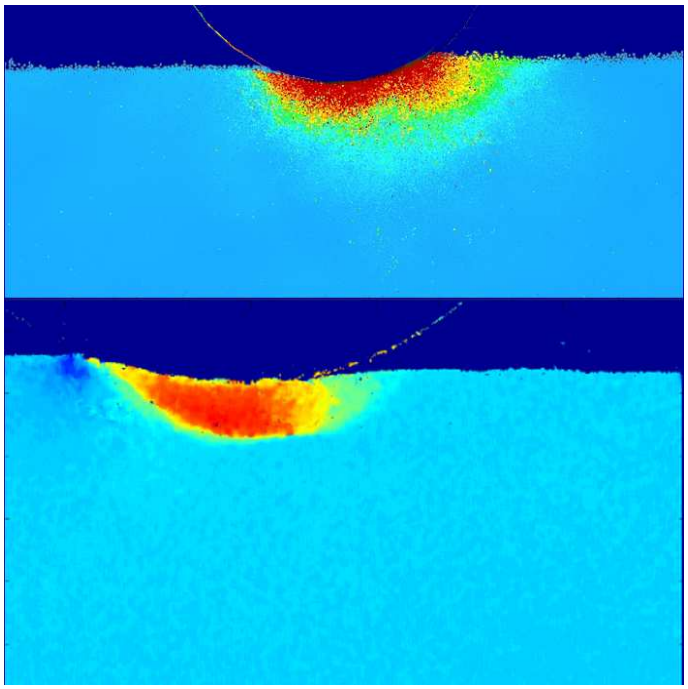

FIGURE 2. **Top:** *View of the velocity wave forms forming under the wheel during a simulation run.* **Bottom:** *View of the velocity wave forms forming under a wheel as it rolls forward. Images is from experimental tests done at CMU [10]*

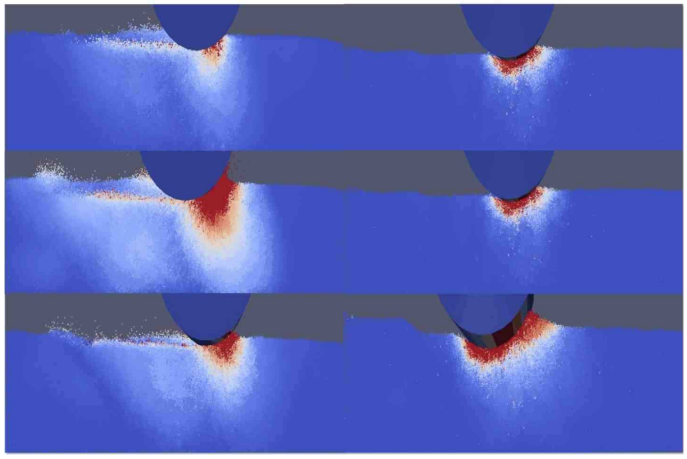

FIGURE 3. *Parametric simulations of wheeled mobility on granular terrains. The first column shows the higher speed results with varying penetration while the second column shows the slower speed results for different penetrations. The deformation field of the granular media is shown in color coding with red being high and blue low. The difference in the deformation fields are clearly noticable*

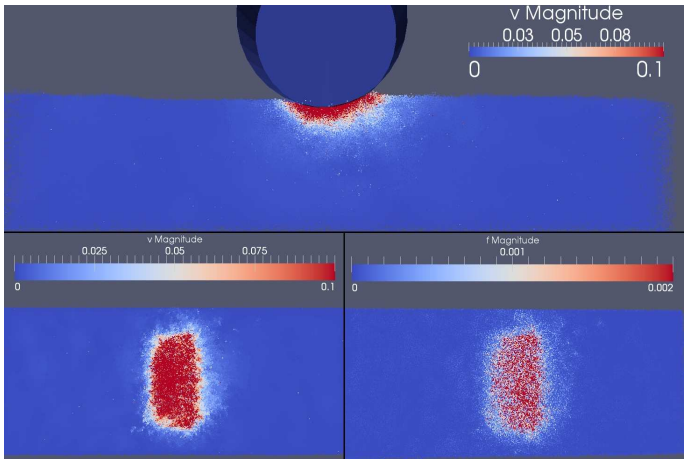

FIGURE 4. *Wheel rolling with 0% slip at 25 cm/s (0.55923 mph) to the right at a depth of 1.5 cm into the bed of granules. A parabolic curve of high velocity granules extends from the front of the wheel to the rear with a large accumulation underneath the moving cylinder.*

speeds used are 10 mph, 15 mph, 20 mph, and 25 mph. For each of these speeds we used three different depths of penetration into the soil. These values were 1 cm, 1.75 cm, and 2.5 cm. Figure 3 shows a montage of the results obtained from these parametric simulations.

In the second set of simulations we investigated how changing values of the coefficient of friction, μ_s, affects the forces in the x and z directions. We ran these simulations for the 20 mph and 15 mph speeds at a depth of 1.75 cm. For both these speeds we varied μ_s by ± 0.2. The results of these simulations are listed in (*Fig. 7*).

In the third set of simulations we investigated how changing values of the coefficient of rolling friction, μ_r, affects the forces in the x and z directions. We ran these simulations for the 20 mph and 15 mph speeds at a depth of 1.75 cm. For both these speeds we varied μ_r by ± 0.2. The results of these simulations are listed in (*Fig. 8*).

As depth and speed increased (*Fig. 6*) so did the $\hat{x}$ and $\hat{z}$ components of the force vector. We also noticed a relationship between F_x/F_z depended on depth the wheel was placed into the material rather then on the speed the wheel was moving. Other interesting results occurred when adjusting the coefficient of friction, μ_s, as shown in (*Fig. 7*). As we increased μ_s the force opposing our motion decreased and as μ_s decreased the force opposing our motion increased. These results make sense if we remember we have kept velocity constant throughout the simulation. Note that this is inter-granular coefficient of friction and not a macroscopic aggregate friction between wheel and terrain. As the coefficient of friction increases, the relative motion between the granules is reduced resulting in a firmer terrain. As the terrain firms up, the displacement field in the granular media reduces and consequently, the resistance to motion arising from terrain deformation reduces. A simplistic interpretation can be that with

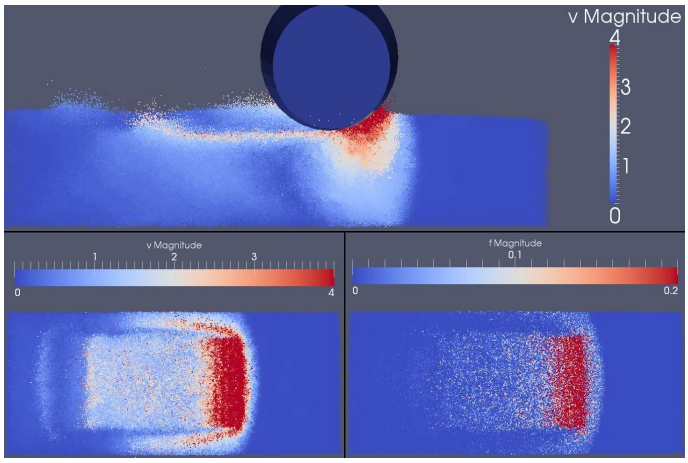

FIGURE 5. *Wheel rolling with 0% slip at 11.176 m/s (25 mph) to the right at a depth of 2.5 cm into the bed of granules. A parabolic curve of high velocity granules is visible extending from the front of the wheel to midway back on the wheel. High velocity granules also extend deep into the bed. Behind the wheel the surface which previously interacted with the cylinder is left disturbed with medium velocity granules.*

increase in the coefficient of friction, the terrain deformation decreases and the wheel approaches near rolling condition. Hence, the reaction force reduces. This type of emergent dynamic behavior needs to be validated through experimentation.

In (*Fig. 4*) the wheel is rotating with 0% slip at 0.55923 MPH toward the right. In this image we also see a clear and distinct parabolic curve. From a top view with the wheel made invisible, the force and velocity fields are also in line with what we would expect to see with the bulk of the effects taking place beneath the cylinder. In (*Fig. 5*) the wheel is also rolling with 0% slip and to the right, but unlike the previous image, it is moving forward at 25 MPH. In this image we also see a distinct parabolic curve. Due to the high speeds, however, this curve is centered more to the front of the wheel and only extends about halfway back on the wheel. We also see this curve of high velocity granules being extended much further into the simulation bed. The surface of the bed is also covered in high velocity granules which have been kicked behind by the rolling wheel. Viewing the force and velocity fields from above shows a parabolic waveform forming in front of the wheel dropping of to the sides of the wheel. Overall the effects we saw with the cylinders interacting with the granular regions was exactly as expected. Our simulation forces were also in line with expectations.

CONCLUSION

We presented the results of parametric simulation of wheeled mobility on granular terrain using massively parallel discrete element method. We reported simulations run on ter-

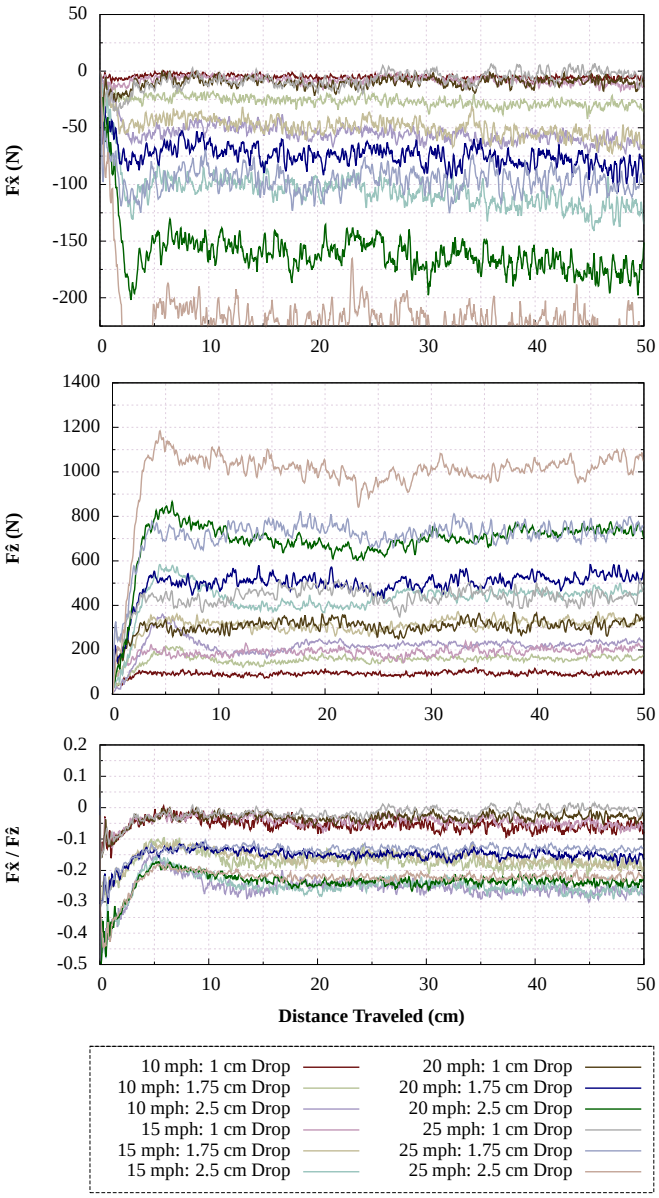

FIGURE 6. *Set of simulations performed with varying wheel depths and speeds. We notice that as the depth and speed increases $F\hat{x}$ and $F\hat{z}$ both increase as well. Also as can be seen in the bottom graph the ratio of $F\hat{x}$ to $F\hat{z}$ only depends on the distance the wheel is dropped into the bed. The material properties for this simulation are listed in (Table 1)*

rains that retain the complexity of natural terrain. Hence these are results of large simulations with millions of granules and the complexity reported here exceeds those of comparable methods reported in literature. Emphasis has been placed on developing single-shot experiments that have a firm predictive basis rather than iteratively turning simulations to match experimental data. The parametric simulations showed the sensitivities of the results

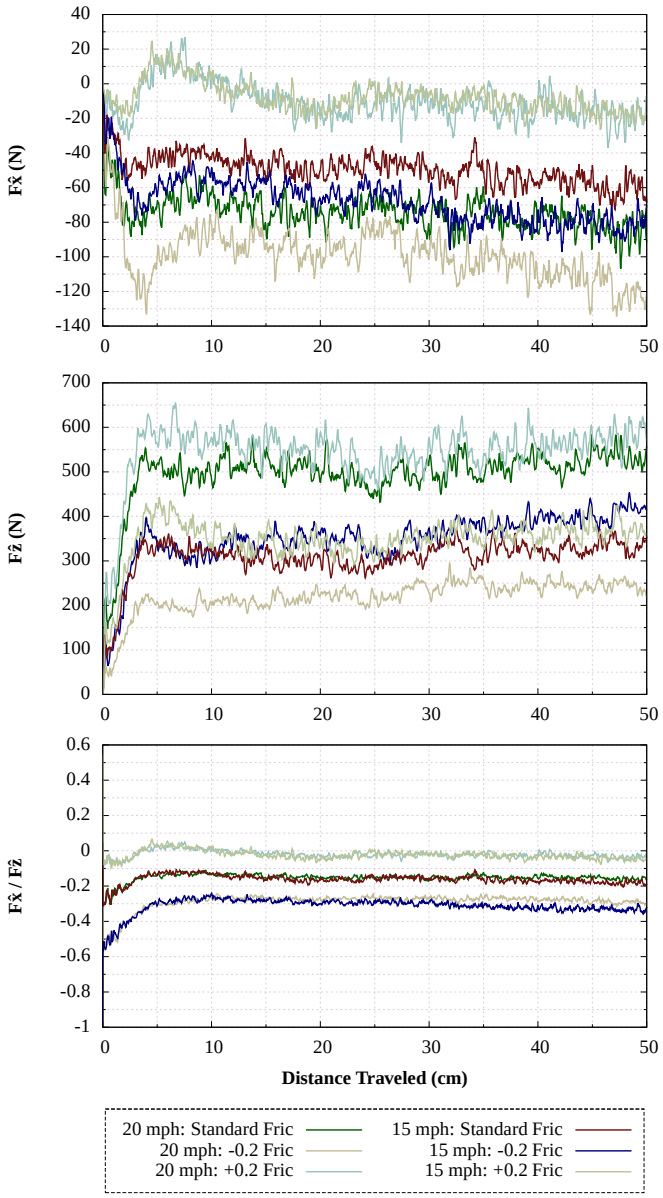

FIGURE 7. *Set of simulations performed with varying values for coefficient of friction. As the frictional force increase the $F\hat{x}$ force decreases and the $F\hat{z}$ force increase. We also notice that the ratio of $F\hat{x}$ to $F\hat{z}$ only depends on the distance the wheel is dropped into the granular bed. The base material properties for this simulation are listed in (Table 1)*

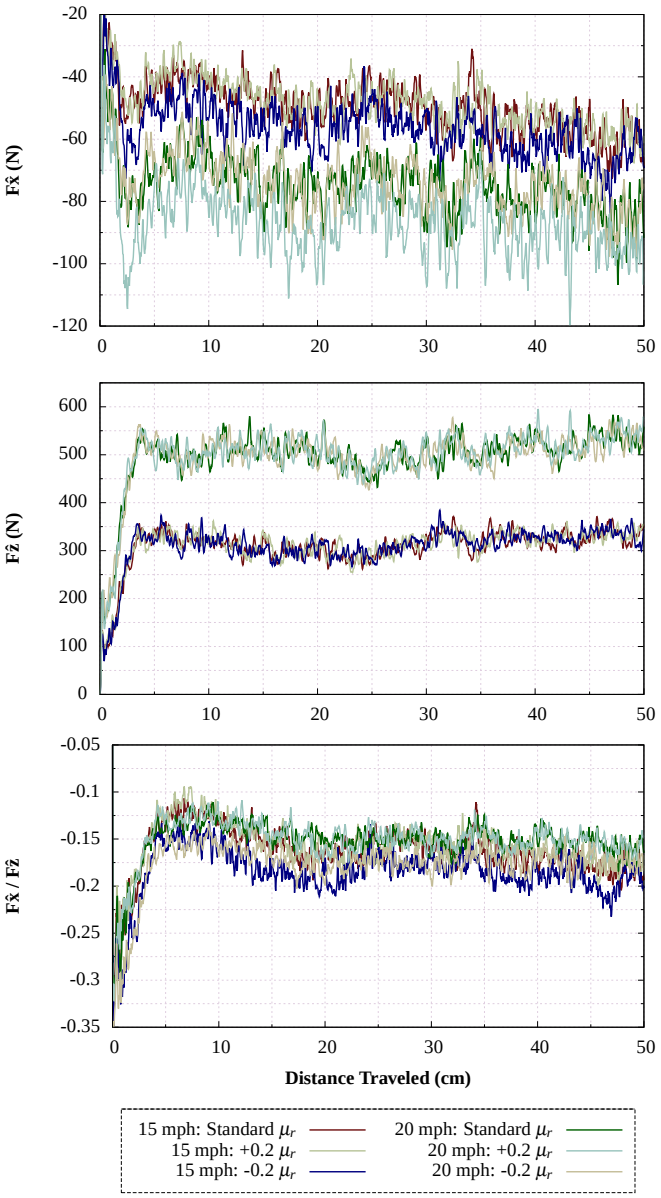

FIGURE 8. *Set of simulations performed with varying values of the coefficient of rolling friction. We notice that, as expected, the value of rolling friction has a negligible effect on any of the forces which tend to remain constant. This is due to the implications of Eq. 11 which says that rolling friction only adds an additional torque contribution. The base material properties for this simulation are listed in (Table 1)*

to parametric perturbations. We found that with DEM modeling we were able to reproduce emergent macroscopic behavior. Qualitative validation is demonstrated by comparing our results against experimentally observed data.

ACKNOWLEDGMENT

The research described in this paper was partially performed at the Jet Propulsion Laboratory, California Institute of Technology, under contract with the National Aeronautics and Space Administration. The authors thank Scott Moreland, Krzysztof Skonieczny and David Wettergreen from Carnegie

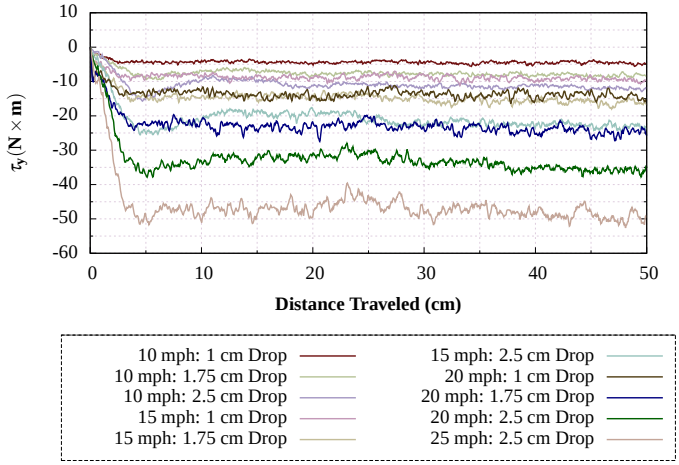

FIGURE 9. *Set of simulations performed with varying values of speed and distance. We notice that, as expected, the toruqe is in the $-\hat{y}$ and it increases with depth and speed. The base material properties for this simulation are listed in (Table 1)*

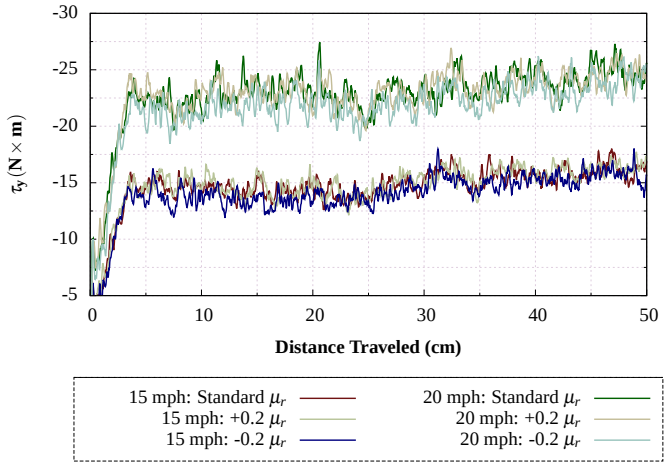

FIGURE 10. *Set of simulations performed with varying values of rotational friction. We notice that, as expected, the torque is in the $-\hat{y}$ and it increases with increasing friction. The base material properties for this simulation are listed in (Table 1)*

Melon University for providing the results of their particle imaging studies of wheeled mobility on granular terrain. The authors thank the DARPA for funding this work through the Adaptive Vehicle Make program and BAE systems Minneapolis for leading the primary proposal effort. The authors also thank Daniel Challou, Chris Wentland and Michael McCullough from BAE systems for their technical collaboration.

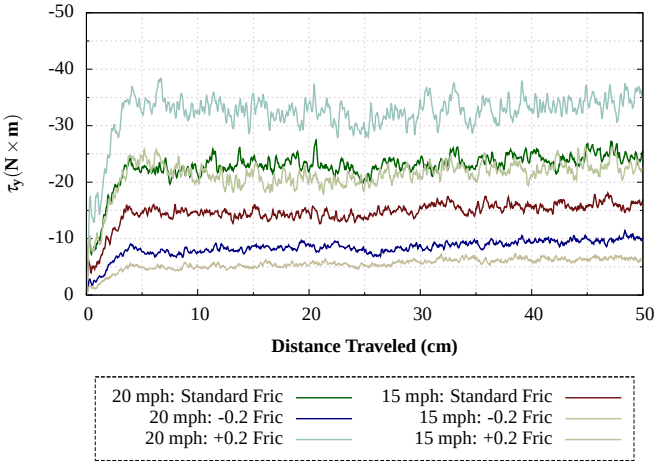

FIGURE 11. *Set of simulations performed with varying values of speed and distance and friction. We notice that, as expected, the torque is in the $-\hat{y}$ and it increases increasing friction. The base material properties for this simulation are listed in (Table 1)*

REFERENCES

[1] Kremmer, M., J. F., 2001. "A computational method for representing boundaries in discrete element modeling". *International Journal for Numerical Methods in Engineering*, ***51 Issue 12***, p. 1407 1421.

[2] Morris, J., and Johnson, S., 2007. "Discrete element modeling". *American Society of Civil Engineers: Journal of Geotechnical and Geoenviormental Engineering*, ***UCRL-JRNL-237027***.

[3] Kloss, C., Goniva, C., Hager, A., Amberger, S., and Pirker, S., 2012. "Models, algorithms and validation for open-source dem and cfd-dem". *An Int. J.*, ***12***(2/3), pp. 140–152.

[4] Plimpton, S. J., 1995. "Fast parallel algorithms for short-range molecular dynamics". *J Comp Phys*, ***117***, pp. 1–19.

[5] Munjiza, J., Bicanic, N., and Owen, D., 1993. "Bsd contact detection algorithm for discrete elements in 2d". In Second International Conference on Discrete Element Methods (DEM).

[6] Perkins, E., and Williams, J., 2001. "A fast contact detection algorithm insensitive to object sizes". *Engineering Computations*, ***18***.

[7] Perkins, E., and Williams, J., 2002. "Generalized spatial binning of bodies of different sizes". In ASCE Discrete Element Methods: Numerical Modeling of Discontinua.

[8] Williams, J., and O'Connor, R., 1995. "A linear complexity intersection algorithm for discrete element simulation of arbitrary geometries". *International Journal for numerical and Analytical Methods in Geomechanics*, ***12***.

[9] Henderson, A., 2007. Paraview guide: A parallel visulization applications. Tech. rep., Kitware Inc.

[10] Moreland, S., Skonieczny, K., Wettergreen, D., Creager, C., and Asnani, V., September, 2011. “Soil motion analysis system for examining wheel-soil shearing”. In International Conference of the International Society for Terrain-Vehicle Systems.

ADDENDUM

On Modeling Tracked Wheels using Massively Parallel Discrete Element Method

Dr. Rudranarayan Mukherjee
Mobility and Robotic Systems Section
Jet Propulsion Laboratory, California Institute of Technology
Pasadena CA 91109
Rudranarayan.M.Mukherjee@jpl.nasa.gov

Introduction

In the body of the main document, we have presented an overview of the underlying methodology of our Discrete Element Method based massively parallel simulations of interactions between compliant granular terrain and wheeled mobility systems. We presented results of parametric simulations that were conducted to understand the effects of speed, penetration and material properties of the terrain on mobility of a cylindrical wheel. This document presents additional results to augment the findings reported in the main document. We aim to transition this addendum to a technical paper in the near future.

Effect of Wheel Profile

Having studied cylindrical wheel motion, we wanted to evaluate the mobility characteristic of a "tracked wheel" that had a more involved geometric profile and was recommended as a track surrogate by our collaborators at BAE Systems. Figure 1 shows a 3D view of the tracked wheel. As observable, this wheel has track pads along its circumference and annular regions between the tracks. We conducted a parametric set of simulations with this wheel similar to the cylindrical wheel i.e. we varied the translational speed of the wheel in zero slip condition to be 10mph, 15mph, 20mph and 25mph. We also varied the penetration or sinkage of the wheel to be 1.0, 1.75 and 2.5 cm into the terrain. We measured the net normal load as well as horizontal load arising on the wheel as it traversed a bed of compacted polydispursed granular media. The material properties on the granular media were set to resemble dry sand. The granular bed was compacted to attain bulk density similar to sand. The simulation consisted of about 2million granules with a distribution of their bounding spheres ranging from 4mm to 0.5mm. The simulations were run on the JPL cluster with an average of 200 processors requiring about 4-5 hours of wall clock time per simulation.

Results:

In the following figures, the normal load and longitudinal loads obtained from the simulations are plotted as a function of time. The vertical axis is load in Newton while the horizontal axis is time in seconds. The figures are arranged in the form of a 4x2 table where the left column corresponds to normal load while the right column corresponds to horizontal load. The rows are ordered in terms of increasing speed i.e. the first row corresponds to 10mph while the final row corresponds to 25mph. Each plot shows three sets of results shown in red, blue and black corresponding to 1cm, 1.75cm and 2.5cm of sinkage.

Normal Load in Newton	Longitudinal Load in Newton
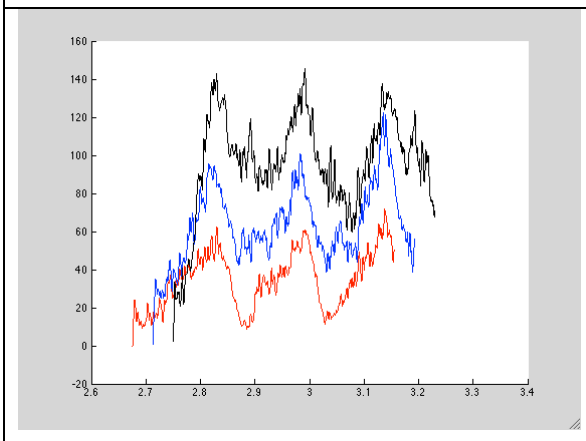	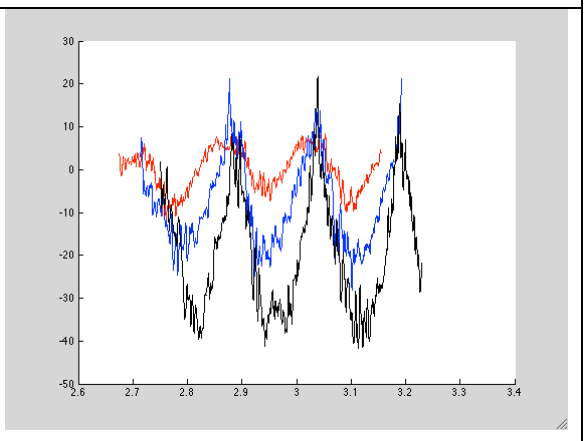

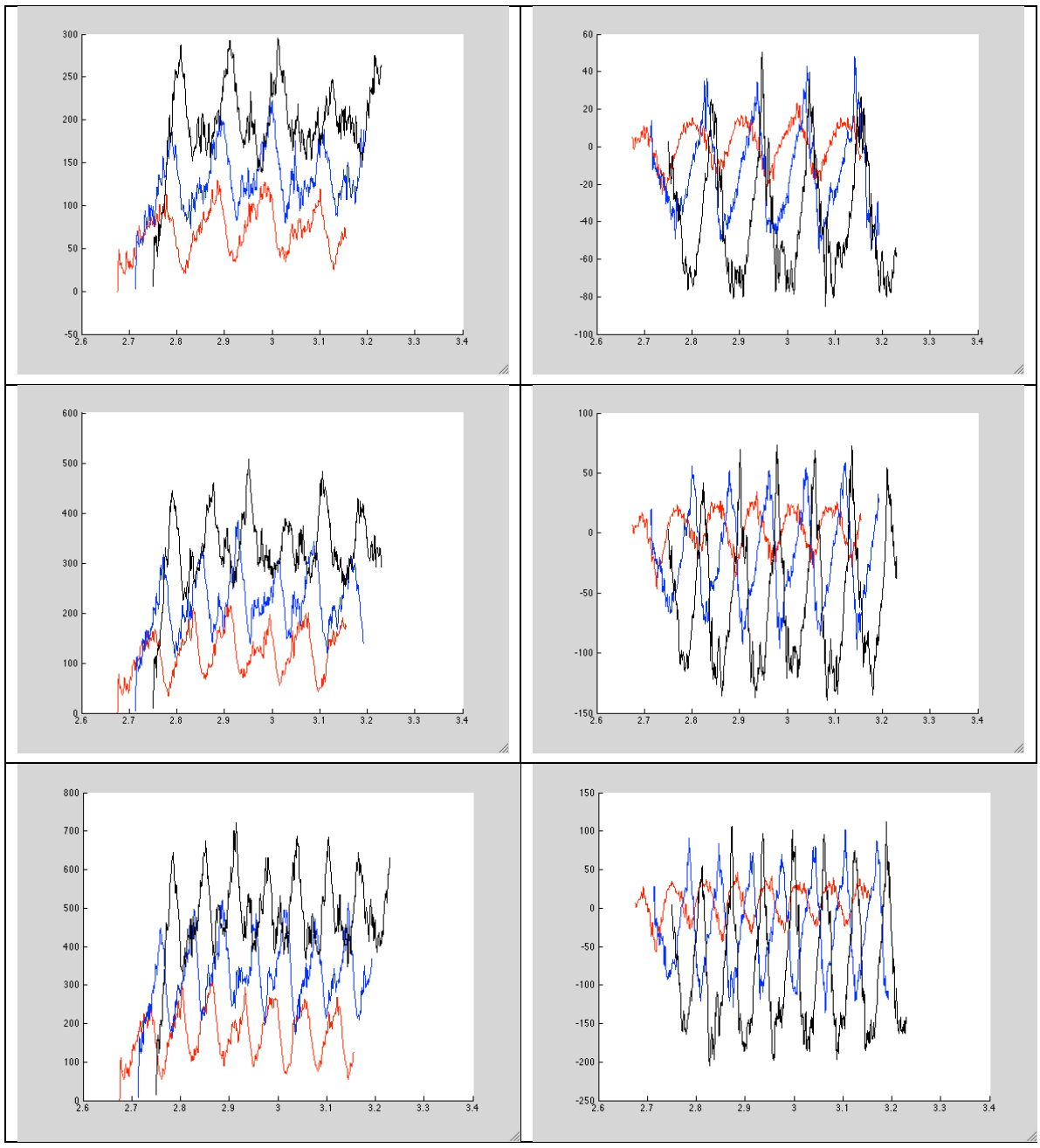

As observed in the figures, the loads vary with the wheel profile. As the wheel rotates, alternately the tracked and annular regions of the wheel come in contact with the terrain. As the track part of the wheel comes in contact with the granular terrain, the extent of compression of the terrain is more compared with the annular region of the wheel. The normal load shows an oscillatory behavior with the same periodicity as that of the pitch of the tracks on the wheel. The additional compression of the terrain also results in an oscillatory longitudinal tractive force on the wheel. As the speed increases, the number of oscillations observed in the figures also increases.

As observed for the cylindrical wheel, higher values of sinkage result in higher normal and longitudinal forces. However the increase in normal force is not linear. In the table below, we plot the factor by which the maximum normal load (left column) and maximum longitudinal load (right column) increase as a function of increase in sinkage value (third row) for the four different speeds (red=10mph, green=15mph,

blue=20mph, black=25mph) as well as the values of the maximum loads (second row). Interestingly, the values are clustered. The 1cm penetration is treated as a base value. Interestingly, the factors of increase in maximum normal load seem to cluster for the different values of speeds. This may be interpreted to mean that the factor of increase in normal load is independent of the speed. However, for the longitudinal loads, this clustering is much less obvious and points to a dependency on the speed. The fourth row of the table shows the maximum normal and longitudinal loads as a function of different speeds for constant penetration.

Normal Load with sinkage	Longitudinal load with sinkage
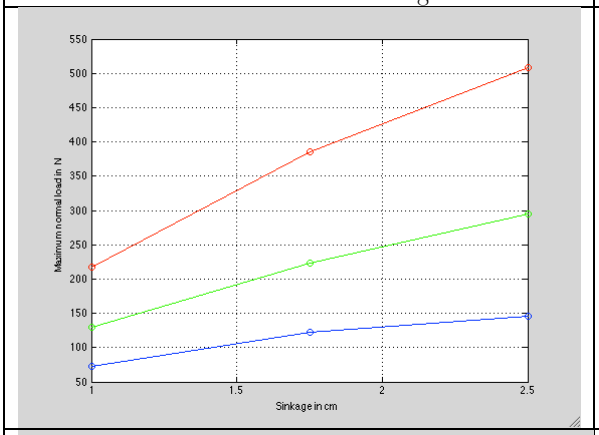	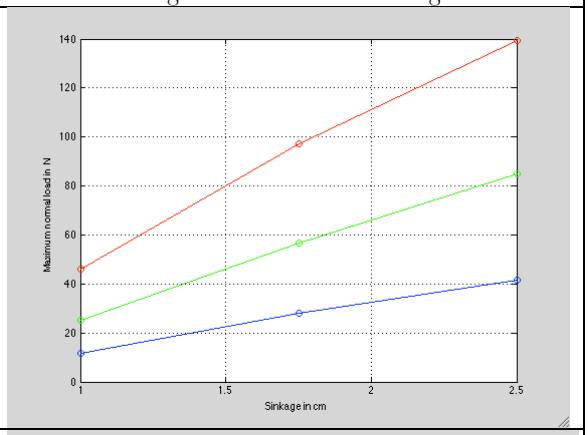
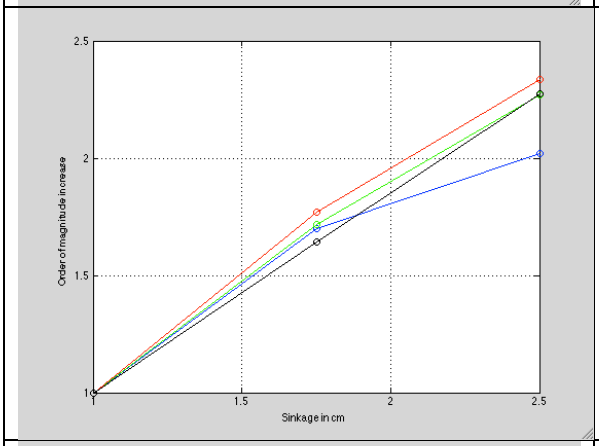	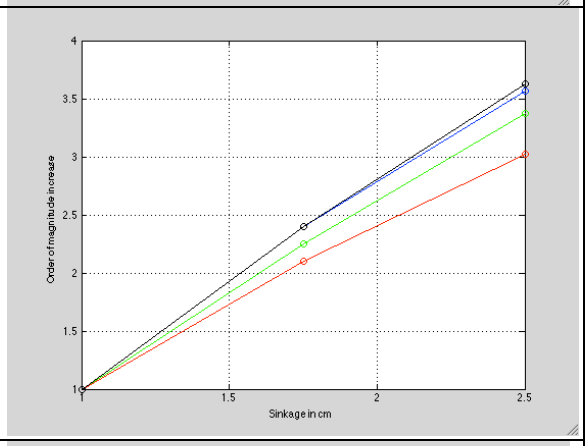
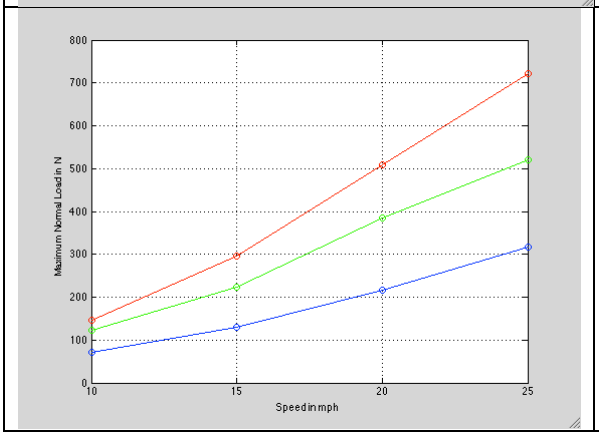	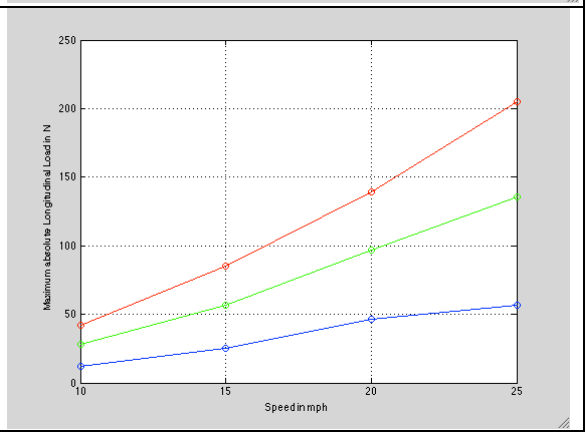

Along with the above quantitative results, we generated full 3D visualizations of the simulation results. The two figures in the following figure show snapshots from these simulations. The figure on the left shows the granules color-coded by their speed. The deformation field is significantly different from the cylindrical

wheel case as the granules conform to the shape of the wheel. In the figure to the right, the wheel is made invisible and the imprint of the wheel on the granular bed is clearly visible.

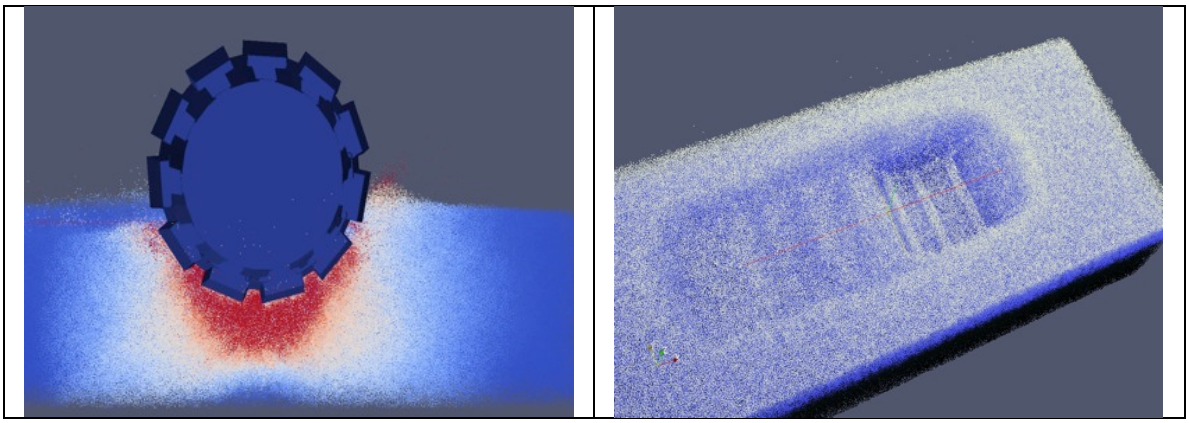

Quantitative Validation of Cylindrical Wheel Results

In the main paper, we only presented qualitative agreement between the images generated by Particle Image Velocimetery and our simulations. In the figure below, we show quantitative agreement between the results. The figure shows the comparison of draw bar pull generated from experimental data at CMU (obtained thru informal collaboration) and that generated by our simulation. As can be seen, the two plots have an identical profile with a peak at -30N and a stable value around -25 and -20N. This demonstrates excellent agreement with the experimental data and validates the simulation. Note that in the experimental data, the sinkage changed in the region between 30-60cm of travel. Hence there is a minor variation between the model and experimental data.

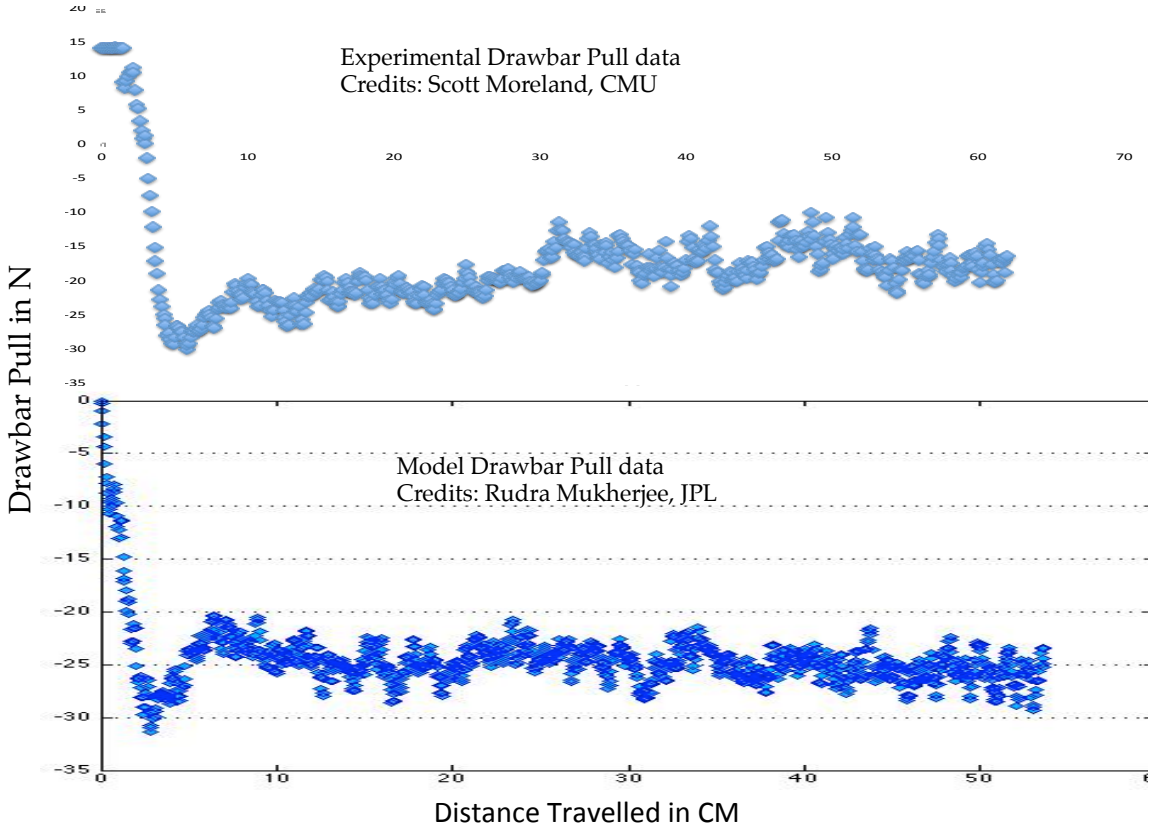

Sloped Terrain

In an effort to quantify mobility on slopes, we have developed granular terrain models for slopes of 10, 15 and 20 degrees. This has been a difficult effort as it has been difficult to get a good compacted slope model. Our simulation results with the slope terrains have generated data that indicate more effort needs to be invested in developing good sloped terrain models. This is currently under continued effort and we aim to resolve this issue shortly.

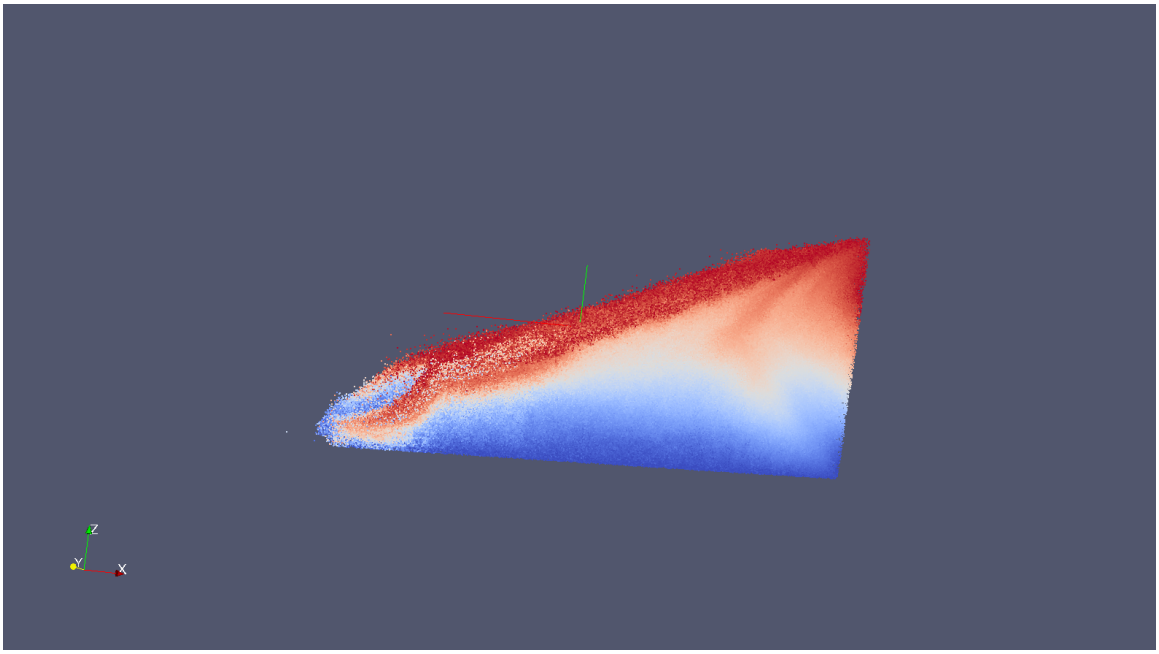

3D visualization of a sloped terrain. The color coding of the granules indicates granule number, blue being low and red being high. It can be observed that there is no clear boundary and the granules have mixed due the compacting process

Acknowledgement

The research described in this paper was performed at the Jet Propulsion Laboratory, California Institute of Technology, under contract with the National Aeronautics and Space Administration. The authors thank Scott Moreland, Krzysztof Skonieczny and David Wettergreen from Carnegie Melon University for providing the results of their particle imaging studies of wheeled mobility on granular terrain. The authors thank the DARPA for funding this work through the Adaptive Vehicle Make program and BAE systems Minneapolis for leading the primary proposal effort. The authors also thank Daniel Challou, Chris Wentland and Michael McCullough from BAE systems for their technical collaboration.